VOLUME 79 SEPARATE No. 211

PROCEEDINGS

AMERICAN SOCIETY
OF
CIVIL ENGINEERS

JULY, 1953

PHOTOELASTIC ANALOGY FOR NON-HOMOGENEOUS FOUNDATIONS

by Allen J. Curtis and F. E. Richart, Jr.

Presented at
Miami Beach Convention
June 16-19, 1953

ENGINEERING MECHANICS DIVISION
{Discussion open until November 1, 1953}

Headquarters of the Society
33 W. 39th St.
New York 18, N. Y.

PRICE $0.50 PER COPY

This paper was published at 1745 S. State Street, Ann Arbor, Mich., by the American Society of Civil Engineers. Editorial and General Offices are at 33 West Thirty-ninth Street, New York 18, N. Y.

PHOTOELASTIC ANALOGY FOR NON-HOMOGENEOUS FOUNDATIONS

Allen J. Curtis*
and
F. E. Richart, Jr.**, Assoc. M. ASCE

Synopsis

This paper deals with the stress distributions in a semi-infinite body in which Poisson's ratio is constant, but the modulus of elasticity varies with depth. The general equations of elasticity for such a point-isotropic material are derived and the validity and limitations of published solutions are discussed. There is shown to be an analogy between the stresses in a constrained slice, which has a modulus of elasticity variable with depth, and the stresses in a plate whose thickness varies in the same manner, providing the state of stress in the plate may be considered to be two-dimensional. Thus the stress distributions beneath infinite line or strip loads on such a foundation may be determined experimentally by the use of photoelasticity. The photoelastic analogy is confirmed by experiments and its use is discussed in detail.

Introduction

For certain problems in the field of soil mechanics, the stress-strain relations in the mass of soil agree reasonably well with Hooke's law. For such conditions, the theory of elasticity will give satisfactory results for stresses and displacements if the properties of the theoretical material are similar to the physical properties of the soil mass.[1] If the soil mass is homogeneous and isotropic as well as elastic, a solution involving only two elastic constants will be applicable. Such solutions as that by Boussinesq,[2] for a concentrated normal load, and that by Cerruti[3], for a concentrated tangential load, each acting on the free surface of a semi-infinite body, have often been used satisfactorily for the study of stresses and deformations beneath foundations. By suitable integration of the equations for stresses, given by these fundamental problems, it has been possible to evaluate the stress distributions beneath line, strip, and areas of the surface which are loaded.

However, the materials encountered in soil mechanics problems are seldom both homogeneous and isotropic. Consequently, actual results are

* Member of the Technical Staff, Research and Development Laboratories, Hughes Aircraft Company, Culver City, California.
**Associate Professor of Civil Engineering, University of Florida, Gainesville, Florida.

1. "Theoretical Soil Mechanics", by K. Terzaghi, John Wiley and Sons, Inc., New York, N. Y., 1943, p. 367.
2. "Applications des Potentiels", by J. Boussinesq, Gauthier-Villars, Paris, 1885.
3. V. Cerruti, Roma, Acc. Lincei, Mem. fis. mat. 1882.

often at variance with the predictions from theory. As a result of this discrepancy, numerous studies have been made, still based on the theory of elasticity, but for which the idealized elastic material is assumed to have properties more nearly like those of soils. For various analyses, the elastic material was assumed to be: (a)homogeneous but aelotropic, that is, having different elastic properties in the horizontal and vertical directions, (b) made up of layered systems, each layer being homogeneous and isotropic, or (c) point isotropic, in which the material is assumed to be isotropic at each point, but is non-homogeneous since the elastic constants vary with their location.

This investigation is concerned with the analyses based on an assumption of point-isotropic materials for which the Poisson's ratio is constant throughout, but for which the modulus of elasticity varies with depth. First the general equations of elasticity are derived for this particular type of point-isotropic material, and these are used to evaluate the existing theoretical studies of the problem. Then by comparing the general equations of elasticity with those equations which represent the stress distribution in a plate of variable thickness, an analogy is established which permits the analysis of stress distributions in the point-isotropic material by the use of a photoelastic model which has a variable thickness.

It is the purpose of this paper to establish the validity of the photoelastic analogy, and to present a study of its usefulness and limitations as an aid for the study of stress distributions in point-isotropic materials.

Notation

The letter symbols used in this paper generally conform to those prescribed in the Manual, "Soil Mechanics Nomenclature", published by the American Society of Civil Engineers, 1941.

Also, in the interest of brevity, the term "solutions" will be used in the following pages to indicate a solution for the stress distribution in a semi-infinite body, due to a surface loading.

In the following discussions, compressive stresses are considered positive as is customary in the study of soil mechanics. Figure 1 shows the coordinate systems used and Figures 2(a) to 2(e) show the directions of positive stresses on the faces of an infinitesimal element of material, as defined by these coordinate systems.

Equations of Elasticity for Point-Isotropic Materials

The theory of elasticity is based on Hooke's law, which may be expressed in a general form by the statement[4], "Each of the six components of stress at any point of a body is a linear function of the six components of strain at the point." This law then gives a possible total of 36 independent elastic constants at each point of the material. However, if the material is assumed to be isotropic, that is, the elastic properties are independent of a rotation of coordinate axes, only two independent elastic constants are obtained at any point. If, in addition, the assumption is made that the material is homogeneous, only two elastic constants are obtained throughout the body. Since the mathematical procedures are greatly simplified by using only two elastic constants, the greater part of the work in the

4. "The Mathematical Theory of Elasticity," by A. E. H. Love, Cambridge University Press, London, 1934, p. 97.

theory of elasticity has been done on the assumptions that the material is isotropic and homogeneous.

For the point-isotropic material, only two independent elastic constants are obtained at each point in the body. However, these two quantities may each have different values at different locations within the elastic body. The values of Poisson's ratio, μ, and the modulus of elasticity, E, will be used in this study as the two independent elastic constants. It will be assumed that Poisson's ratio has the same value throughout the body, but that the modulus of elasticity is a function of depth only. Since the modulus of elasticity in shear, G, is then equal to E multiplied by a constant, this term may be used equally well in the subsequent equations.

These foregoing assumptions regarding the elastic constants in no way affect the usual stress-strain relations, since these are concerned with the conditions at a point of the body. Also the strain-displacement equations are unaffected by the assumed variation of the elastic constants.

The equilibrium equations in terms of stress express the equations of statics which must be satisfied throughout a body. Thus again, variations of elastic constants cannot affect the equations in this form. In terms of stresses, the equations of equilibrium may be written,

$$\frac{\partial \sigma_x}{\partial x} + \frac{\partial \tau_{xy}}{\partial y} + \frac{\partial \tau_{xz}}{\partial z} + X = 0 \quad ---(x,y,z) \tag{1}$$

for Cartesian coordinates. The (x, y, z) to the right of the equation indicate that similar equations, for the other coordinate directions, may be written by a cyclic interchange of subscripts.

In the type of problem under consideration, the only body forces encountered will be the gravity loading of the soil. However, it will be shown that the differential equations to be satisfied in this point-isotropic medium are linear, so that the law of superposition is valid. Thus, the effects due to gravity loading may be added separately to any solution obtained; consequently the body forces will be neglected in the following pages.

In addition to the equilibrium equations, boundary conditions, and stress-strain relations a complete solution of a problem by use of the theory of elasticity must also satisfy the equations of compatibility. These equations, when satisfied, guarantee that the displacements in the body are single-valued at every point. In terms of strains, the compatibility equations for a three-dimensional system are,

$$\frac{\partial^2 \varepsilon_x}{\partial y^2} + \frac{\partial^2 \varepsilon_y}{\partial x^2} = \frac{\partial^2 \gamma_{xy}}{\partial x \partial y} \quad ---(x,y,z) \tag{2}$$

$$\frac{2\partial^2 \varepsilon_x}{\partial y \partial z} = \frac{\partial}{\partial x}\left[-\frac{\partial \gamma_{yz}}{\partial x} + \frac{\partial \gamma_{zx}}{\partial y} + \frac{\partial \gamma_{xy}}{\partial z}\right] \cdots (x, y, z) \tag{3}$$

These equations are independent of the elastic constants, E, and μ, in this form. However, one convenient method of attack for solving problems in elasticity is to transform Eqs. (2) and (3) into terms of stresses, by making use of the stress-strain relations and equilibrium equations.[5] When the boundary conditions are known in terms of stresses, as is the case for the type of problem under consideration, this seems to be preferable.

In accordance with the usual practice, the z-direction has been chosen as the direction of increasing depth, so that E or G is a function of z only, that is,

$$\frac{\partial E}{\partial x} = \frac{\partial G}{\partial x} = \frac{\partial E}{\partial y} = \frac{\partial G}{\partial y} = 0 \tag{4}$$

Substituting the stress-strain relations into Eqs. (2) and (3), and using the equilibrium equations to eliminate shearing stresses, the three-dimensional equations of compatibility in terms of stresses become:

$$\left[\Delta\theta - \Delta\sigma_z - \frac{\partial^2 \theta}{\partial z^2}\right] - \frac{\mu}{1+\mu}\left[\Delta\theta - \frac{\partial^2 \theta}{\partial z^2}\right] = 0 \tag{5}$$

$$\left[\Delta\theta - \Delta\sigma_x - \frac{\partial^2 \theta}{\partial x^2}\right] - \frac{\mu}{1+\mu}\left[\Delta\theta - \frac{\partial^2 \theta}{\partial x^2}\right] - 2\left[\frac{\partial}{\partial z}\left\{\sigma_y - \frac{\mu}{1+\mu}\theta\right\} - \frac{\partial \tau_{yz}}{\partial y}\right]\frac{\partial \ln G}{\partial z} + \left[\sigma_y - \frac{\mu}{1+\mu}\theta\right]\left[\left(\frac{\partial \ln G}{\partial z}\right)^2 - \frac{\partial^2 \ln G}{\partial z^2}\right] = 0 \tag{6}$$

5. "Theory of Elasticity," by S. Timoshenko and J. N. Goodier, McGraw-Hill 1951, p. 230.

$$\left.\begin{aligned}&\left[\Delta\theta - \Delta\sigma_y - \frac{\partial^2\theta}{\partial y^2}\right] - \frac{\mu}{1+\mu}\left[\Delta\theta - \frac{\partial^2\theta}{\partial y^2}\right] \\ &-2\left[\frac{\partial}{\partial z}\left\{\sigma_x - \frac{\mu}{1+\mu}\theta\right\} - \frac{\partial \tau_{xz}}{\partial x}\right]\frac{\partial \ln G}{\partial z} \\ &+\left[\sigma_x - \frac{\mu}{1+\mu}\theta\right]\left[\left(\frac{\partial \ln G}{\partial z}\right)^2 - \frac{\partial^2 \ln G}{\partial z^2}\right] = 0\end{aligned}\right\} \quad (7)$$

$$\Delta \tau_{yz} + \frac{1}{1+\mu}\frac{\partial^2\theta}{\partial y \partial z} + \left[\frac{\partial \tau_{xy}}{\partial x} - \frac{\partial}{\partial y}\left(\sigma_x - \frac{\mu}{1+\mu}\theta\right)\right]\frac{\partial \ln G}{\partial z} = 0 \quad (8)$$

$$\Delta \tau_{xz} + \frac{1}{1+\mu}\frac{\partial^2\theta}{\partial x \partial z} + \left[\frac{\partial \tau_{xy}}{\partial y} - \frac{\partial}{\partial x}\left(\sigma_y - \frac{\mu}{1+\mu}\theta\right)\right]\frac{\partial \ln G}{\partial z} = 0 \quad (9)$$

$$\left.\begin{aligned}&\Delta \tau_{xy} + \frac{1}{1+\mu}\frac{\partial^2\theta}{\partial x \partial y} \\ &+\left[\frac{\partial \tau_{xz}}{\partial y} + \frac{\partial \tau_{yz}}{\partial x} - \frac{2\,\partial \tau_{xy}}{\partial z}\right]\frac{\partial \ln G}{\partial z} \\ &+ \tau_{xy}\left[\left(\frac{\partial \ln G}{\partial z}\right)^2 - \frac{\partial^2 \ln G}{\partial z^2}\right] = 0\end{aligned}\right\} \quad (10)$$

In Eqs. (5) through (10), $\Delta = \left(\frac{\partial^2}{\partial x^2} + \frac{\partial^2}{\partial y^2} + \frac{\partial^2}{\partial z^2}\right)$ = Laplace's θ operator, θ denotes the sum of the principal stresses, and ln G designates the natural logarithm of the shear modulus.

Adding Eqs. (5), (6), and (7), and again using the equilibrium equations to eliminate shear stresses, the following equation is obtained:

$$\Delta\theta - 2\frac{\partial\theta}{\partial z}\frac{\partial \ln G}{\partial z} + \left[\theta - \frac{1+\mu}{1-\mu}\sigma_z\right]\left[\left(\frac{\partial \ln G}{\partial z}\right)^2 - \frac{\partial^2 \ln G}{\partial z^2}\right] = 0 \tag{11}$$

It is evident that if G is constant, the above compatibility equations reduce to those given by Timoshenko and Goodier.[6] Moreover, all these equations are linear so that the stresses and displacements due to different boundary conditions may be superposed.

In the system which corresponds to plane strain in the x - z plane, the compatibility relations are reduced from six to one, since

$$\varepsilon_y = \gamma_{yz} = \gamma_{yx} = \frac{\partial}{\partial y} = 0 \tag{12}$$

By substituting these relations into Eqs. (2) and (3), and using the stress-strain and equilibrium equations, the compatibility equation in terms of stress is determined as follows for plane strain:

$$\Delta\theta' - 2\frac{\partial\theta'}{\partial z}\frac{\partial \ln G}{\partial z} + \left[\sigma_x - \frac{\mu}{1-\mu}\sigma_z\right]\left[\left(\frac{\partial \ln G}{\partial z}\right)^2 - \frac{\partial^2 \ln G}{\partial z^2}\right] = 0, \tag{13}$$

where $\theta' = \sigma_x + \sigma_z$.

For the case of plane stress, a slice is considered to be in a state of plane stress if the faces of the slice are free of surface tractions, and if it is thin enough in comparison with its other dimensions so that variations of stress through the thickness may be considered negligible.

This condition requires that for plane stress in the x - z plane,

$$\sigma_y = \tau_{xy} = \tau_{zy} = \frac{\partial}{\partial y} = 0 \tag{14}$$

Under these assumptions, the compatibility relations reduce to,

$$\frac{\partial^2 \varepsilon_x}{\partial z^2} + \frac{\partial^2 \varepsilon_z}{\partial x^2} = \frac{\partial^2 \gamma_{xz}}{\partial x \partial z}, \tag{15}$$

6. See footnote 5, p. 231.

and $$\frac{\partial^2 \varepsilon_y}{\partial x^2} = \frac{\partial^2 \varepsilon_y}{\partial z^2} = \frac{\partial^2 \varepsilon_y}{\partial x \partial z} = 0 \,. \tag{16}$$

Eqs. (16) are satisfied if

$$\varepsilon_y = -\frac{\mu\theta}{E} = ax + by + c \,. \tag{17}$$

It is customary to solve plane stress problems neglecting Eqs. (16) which also involves disregarding two shear stress-strain relations which relate Eqs. (14) and (16). Reissner[7] has shown that the error due to this simplification is small if the change in the normal stresses is moderate in a distance equal to the thickness of the slice. In addition, by integrating the correction to the stresses obtained in this manner, across the thickness of the plate, the result is zero. Consequently in photoelastic work the fringe patterns will agree with this average stress distribution.

The compatibility equation for the case of plane stress in the x - z plane may be transformed into terms of stress to give:

$$\Delta\theta' - 2\frac{\partial\theta'}{\partial z}\frac{\partial \ln G}{\partial z} + \left[\sigma_x - \mu\sigma_z\right]\left[\left(\frac{\partial \ln G}{\partial z}\right)^2 - \frac{\partial^2 \ln G}{\partial z^2}\right] = 0 \tag{18}$$

The differential equations which have been derived above for a point-isotropic material could be put in many forms, for example in terms of Airy's stress function for the two-dimensional cases. It is evident that the variable modulus of elasticity greatly complicates the equations to be satisfied, and there seems to be little hope for mathematical solutions of practical value except for special forms of G, some of which will be considered in the following section.

Inspection of these equations shows the following points. First, all the equations are linear, so that the solutions for different surface loadings or displacements may be superposed. Thus the solutions for a concentrated force or a line load of infinite length are again fundamental solutions for the three- and two-dimensional problems respectively. Secondly, it is the rate of change of ln G (or ln E) which influences the stress distribution, rather than the actual value or rate of change of G (or E). Finally, the solutions of two-dimensional problems depend on the value of Poisson's ratio, in contrast to the solutions ordinarily obtained under the assumption of a constant modulus.

7. "On the Calculation of Three-Dimensional Corrections for the Two-Dimensional Theory of Plane Stress," by E. Reissner, Proc. 15th Semi-Annual Eastern Photoelasticity Conference, June 1942, p. 23.

Previous Solutions for Point-Isotropic Materials

Since the solutions for homogeneous isotropic materials are well known, they will serve as convenient standards of comparison for solutions based on different types of materials. For a normal point load acting on the surface of the semi-infinite homogeneous isotropic body, Boussinesq's equations for the stresses are available in various books dealing with the theory of elasticity.[8]

Boussinesq's equations for stresses, for the condition that $\mu = 1/2$, correspond to what has been called a "rectilinear" transmission of stress. By this it is meant that the direction of any ray emanating from the point of load application is in the direction of the only non-vanishing principal stress. However, the term "radial transmission of stress" seems to be more descriptive and will be used in the following discussion to designate this particular stress distribution. For this stress distribution, the only principal stress not equal to zero, is:

$$\sigma_R = \frac{3P}{2\pi} \frac{\cos\psi}{R^2} = \frac{3P}{2\pi} \frac{z}{R^3} \tag{19}$$

It is interesting to note that for any value of Poisson's ratio the resultant of the normal and shear stresses on an element of a horizontal plane, passes through the point of application of the load. This is evident from the relation,

$$\frac{\sigma_z}{\tau_{rz}} = \cot\psi = \frac{z}{\rho} \tag{20}$$

Fröhlich[9] has shown that for any value of Poisson's ratio, the direction of the maximum principal stress does not vary appreciably from the radial (R) direction until the angle ψ becomes large. In this region however, the stresses are now small. Accordingly he assumed a radial transmission of stress as an approximation for any value of Poisson's ratio, and for any type of variation of E.

The equation for the equilibrium of the region beneath the load establishes a stress distribution,

$$\sigma_R = \frac{nP}{2\pi R^2} \cos^{n-2}\psi \ , \tag{21}$$

8. See footnote 5, p. 364.
9. "Druckverteilung im Baugrund," by O. K. Fröhlich, J. Springer, Vienna, 1934.

where n is an arbitrary parameter. Since this is the only principal stress not equal to zero, the stresses expressed in terms of cylindrical coordinates are obtained directly as,

$$\sigma_z = \frac{nP}{2\pi R^2} \cos^n \psi ,$$

$$\sigma_\rho = \frac{nP}{2\pi R^2} \cos^{n-2} \psi \sin^2 \psi , \qquad (22)$$

and $$\tau_{\rho z} = \frac{nP}{2\pi R^2} \cos^{n-1} \psi \sin \psi .$$

For values of $n > 2$, the above stresses satisfy the differential equations of equilibrium and the boundary conditions.

To obtain the appropriate value of n, Fröhlich determined the value which made the strain energy a minimum throughout a hemispherical shell, of radii R_2 and R_1 ($R_2 > R_1$), beneath the load. By introducing the expression for the variation of the modulus,

$$E = k z^w \qquad (23)$$

the strain energy of the region was found to be a minimum for $n = w + 3$. For a constant modulus, $n = 3$, and substitution of this into Eq. (21) gives the Boussinesq stress distribution for $\mu = 1/2$, (Eq. (19)). For a modulus increasing linearly with depth, $n = 4$.

The value of n obtained above is independent of the inner and outer radii of the shell; consequently the result is valid for a semi-infinite body, providing a small region about the singularity under the load is excluded in the usual way.

Fröhlich has thus obtained a stress distribution which satisfies the boundary conditions, the differential equations of equilibrium, and makes the strain energy a minimum for the assumed form of the stress distribution. However, this does not mean that the solution is correct, since the compatibility relations have not been fulfilled. The minimizing of the strain energy does not replace these relations; in effect, it makes the deviation from the correct solution as small as possible for the assumed stress distribution.

The form of Eq. (21) has suggested the interpretation of the quantity, n, as a "stress concentration factor." This concept permits an evaluation of the influence of non-homogeneity of the material upon the stress distribution beneath the load. Cummings[10] has integrated Eq. (21), to obtain the values of σ_z on the axis of symmetry due to a uniform and parabolic intensity of pressure distributed over a circular area of the surface. He used values of n equal to 3 and 6, and showed that the stresses computed using $n = 6$ and the parabolic surface load distribution agreed best with experimental data, at depths greater than the radius of the loading area. However, he did not mention the elastic constants of the material used, and concluded that the equations of elasticity must be modified before they can

10. "Distribution of Stresses Under a Foundation," by A. E. Cummings, Transactions, ASCE, V. 101, 1936, p. 1072.

be applied to soils. As will be shown later, the elastic constants of the material determine the value of n which must be used in Fröhlich's equations to give a correct solution.

In the discussions of Cummings' paper, various investigations presented correlations between this quantity, n, and properties of soils. D. P. Krynine derived an expression,

$$n = 2 + \frac{1}{K} \quad , \tag{24}$$

in which K is the coefficient of earth pressure at rest, defined as the ratio of horizontal to vertical pressure at a point. This ratio may also be determined as,

$$K = \frac{\sigma_x}{\sigma_z} = \frac{\mu}{1-\mu} \, , \tag{25}$$

at any point in a semi-infinite elastic, isotropic mass of material which is loaded by its own weight. Thus, Eq. (24) can be rewritten as,

$$n = 2 + \frac{1-\mu}{\mu} = 1 + \frac{1}{\mu} \, . \tag{26}$$

Krynine, N. M. Newmark, and A. Casagrande each pointed out the possibility that n might vary with depth in actual soils. Also it was noted that layers of different stiffness affected this stress concentration factor. Thus the modulus of elasticity of the material, and more specifically its mode of variation with depth, as well as Poisson's ratio, were believed to have a significant correlation with the factor, n.

Further studies of stresses in non-homogeneous foundations were made by Ohde.[11] He examined Fröhlich's solution with respect to the question of the compatibility relations, and employed an equation of compatibility corresponding to Eq. (11). He considered moduli of elasticity given by:

$$E = k(z + z_o)^{\omega} \, , \tag{27}$$

and

$$E = k z^{\omega} \, . \tag{28}$$

For these moduli, Eq. (11) becomes, respectively,

$$\Delta\theta - \frac{2\omega}{(z+z_o)} \frac{\partial\theta}{\partial z} + \frac{\omega(1+\omega)}{(z+z_o)^2} \left[\theta - \frac{m+1}{m-1} \sigma_z\right] = 0 \, , \tag{29}$$

11. "Zur Theorie der Druckverteilung im Baugrund," by J. Ohde, Der Bauingenieur, Vol. 20, 1939, p. 451.

and

$$\Delta\theta - \frac{2w}{z}\frac{\partial\theta}{\partial z} + \frac{w(1+w)}{z^2}\left[\theta - \frac{m+1}{m-1}\sigma_z\right] = 0, \tag{30}$$

in which $m = \frac{1}{\mu}$. Ohde stated that Eq. (30) is satisfied by Fröhlich's solution (Eq. (21)) if,

$$n = w+3 = m+1 = 1+\frac{1}{\mu} \tag{31}$$

For a correct solution, all six compatibility relations must be satisfied. Substitution of the stresses, obtained from Fröhlich's solution, into Eqs. (5) through (10) shows that they are satisfied for a modulus given by Eq. (28), if Eq. (31) is satisfied.

The significant point concerning Eq. (31) is that it defines a definite relationship between Fröhlich's "stress concentration factor," (n), Poisson's ratio, and the exponent w which describes the manner of variation of the elastic modulus with depth. Thus for a constant modulus, w = O, and Eq. (31) gives n = 3 and $\mu = 1/2$. For these conditions, Fröhlich's solution is identical with that of Boussinesq. For w = 1, a modulus increasing linearly with depth is defined, and correct results are obtained from Fröhlich's solution only if Poisson's ratio is 1/3.

Fröhlich has also obtained solutions (See Table 3) in a similar manner for the two-dimensional problem. Calculations show that this solution again satisfies the compatibility relation for plane strain (Eq. (13)) under the same conditions as for the three-dimensional case. This is to be expected since the two-dimensional solution is merely an integration of the three-dimensional solution. By further integrations, solutions corresponding to any given normal surface loading can be obtained.

Ohde also derived the correct solution for a concentrated force, W, applied in the direction of the x-axis at a point on the surface of the semi-infinite body. The stress distribution is defined by:

$$\sigma_R = (n-2)\frac{nW}{2\pi R^2}\cos\phi\sin\psi\cos^{n-3}\psi . \tag{32}$$

For a correct solution, the value of n used in Eq. (32) must be determined from Eq. (31) if the modulus of elasticity is defined by Eq. (28). For n = 3, the above equation becomes identical to the one given by Cerruti.

The solution derived by Fröhlich for the condition involving a modulus of elasticity increasing linearly with depth (E = kz), has been confirmed by Borowicka.[12] By assuming the stresses and displacements in terms of an infinite power series with unknown constant coefficients, he obtained a solution for the case of the point load which may be evaluated for any value of

12. "Die Druckausbreitung im Halbraum bei linear zunehmenden Elastizitätsmodul" by H. Borowicka, Ing. Archiv., Vol. 14, 1943, p.75.

Poisson's ratio. For two values of μ, the series degenerate to single terms. For $\mu = 1/3$, Frohlich's solution is obtained, and for $\mu = 1/2$, the result is identical with the Boussinesq solution. Since Borowicka worked directly with displacements, that is, the basic equation of elasticity, it was unnecessary to use the compatibility equations. Substitution of the stresses he obtained using $\mu = 1/3$ or $\mu = 1/2$ into the compatibility equations shows that these are satisfied by his solution. Borowicka's results, shown in Table 1, indicate that the values of the vertical stress on the axis of loading, depend very much upon the value of Poisson's ratio. For a change in Poisson's ratio from 1/2 to zero, a corresponding increase of stress of about 76% occurs, at any given depth. Consequently, the use of Fröhlich's solution may give a considerable error if the conditions of Eq. (31) are not satisfied.

In a further study, Borowicka[13] presented a solution for the two-dimensional problem for which the modulus of elasticity of the material was assumed to be,

$$E = \frac{k}{z}, \tag{33}$$

which corresponds to an infinitely rigid top surface. For this case, the last term of the compatibility relation for plane strain (Eq. 13) is equal to zero, so that the stress distribution is independent of Poisson's ratio. The stress distribution is radial, and the only principal stress not equal to zero is given by,

$$\sigma_r = \frac{4g}{\pi^2} \cdot \frac{1}{z} \arctan\frac{z}{x} = \frac{4g}{\pi^2} \frac{\left(\frac{\pi}{2} - \theta\right)}{z} \tag{34}$$

Along the axis of loading, this gives the same value as the Flamant[14] solution for constant E.

The condition that Eq. (31) must be satisfied by the value of n to be used in Fröhlich's solution, does not imply that n must be an integer. However, n must be equal to, or greater than 3 since Poisson's ratio cannot be greater than 1/2. The expression for the modulus of elasticity,

$$E = k z^{\frac{1}{2}} \tag{35}$$

requires the use of n = 3.5, and $\mu = 0.4$ in the Fröhlich equation in order to arrive at a correct solution. The modulus described in Eq. (35) has been used as an approximation for the study of stress distributions beneath a footing on granular soils. A solution for stresses and displacements, based on this variation of the elastic modulus, was given by Hruban.[15] He

13. "Die Druckausbreitung in einer Halbscheibe bei mit der Tiefe abnehmenden Elastizstatsmodul," by H. Borowicka, Oest. Ing. Archiv., Vol. 2, 1948, p. 360.
14. See footnote 5, p. 85 for a discussion of this solution.
15. "The Influence of the Heterogeneity of the Soil Mass on its Deformation", by K. Hruban, Proceedings of the Second International Conference on Soil Mechanics and Foundation Engineering, Rotterdam, 1948, Vol. 1, p. 123.

considered both normal and tangential loadings, acting on a point, a strip, or a circular area of the surface of the body.

The preceding section has established the validity and/or limitations of the known solutions for point isotropic materials. In addition, it has provided some check on the derivations of the general equations of elasticity, inasmuch as Ohde and Borowicka arrived at the same equations for particular types of variable moduli.

The available results for the vertical stress, σ_z, are summarized in Tables 2 and 3.

The Photoelastic Analogy

In the previous sections, the effects on the stress distributions due to a modulus of elasticity varying with depth have been examined from a mathematical point of view, and the differential equations which must be satisfied have been derived.

It is instructive to consider the problem from a physical viewpoint also. Data from soil tests indicate that elastic soils often exhibit a modulus which increases with depth. Such soils may perhaps be considered as made up of an infinite number of thin horizontal layers of homogeneous isotropic materials. With increasing depth, each layer is somewhat more rigid so that a given uniform pressure on two adjacent layers will produce a smaller contraction in the lower layer. Such a physical concept has been used previously by Terzaghi,[16] and by Newmark,[17] as a basis for methods of estimating the stress distribution in non-homogeneous foundations. By these methods the vertical thicknesses of layers were adjusted in proportion to their relative stiffnesses, and then the Boussinesq solution was applied to this transformed material.

A similar physical interpretation of the problem may be gained by considering a thin slice from a semi-infinite body of homogeneous, isotropic material which is loaded along a region of the free surface. If the slice has a constant thickness, then the stress distribution will correspond to that produced by an infinite line or strip loading on the semi-infinite body. Now let the thickness of the slice vary as a function of depth only, and assume it increases with depth. If the thickness changes smoothly, and not too rapidly, then it is reasonable to expect that the stress distribution may be considered to be two-dimensional, and that the variations of stress through the thickness are negligible. The slice may thus be considered to be an infinite number of thin strips, each strip being somewhat wider with increasing depth. If a uniform pressure is applied over the top surface of such a slice, the value of stress and accompanying vertical contractions will decrease with depth. Thus there appears to be a physical analogy between the soil with a varying modulus, and the slice with varying thickness. It will now be shown that this relationship holds mathematically, thus establishing a method for determining the stress distribution in a point-isotropic material by the use of photoelasticity.

The stress distribution in a semi-infinite body produced by a line or strip load on the surface is analyzed as a problem of plane strain. However, a photoelastic model represents a problem of plane stress. In order to use the results from photoelastic tests to describe stress distributions

16. "Bodenpressung und Bettungsziffer", by K. Terzaghi, Oesterreichische Bauzeitung, No. 25, 1932.
17. Footnote, 10, see Discussion by N. M. Newmark, p. 1115.

for a case of plane strain, it is necessary to use the plane stress - plane strain, or free slice - constrained slice, analogy which has been discussed by Westergaard[18] and by Mindlin and Salvadori.[19]

For homogeneous isotropic materials, this analogy states that any problem in plane stress may be considered as a problem in plane strain, or vice versa, provided that a suitable change in the elastic constants is made. If the region under consideration, (a) is not subjected to body forces, or is subjected to body forces which are harmonic, (b) is simply connected, and (c) is not subjected to thermal stresses, then the stress distribution is independent of the elastic constants, and is the same for free and constrained slices. The problem under consideration using point-isotropic materials satisfies conditions (a), (b), and (c) above, but it is not independent of the elastic constants due to the change in the compatibility equation. (see Eqs. (13) and (18)). It is therefore necessary to determine what changes in elastic constants are necessary for the analogy to hold for point-isotropic materials.

Consider a plane stress system with elastic constants E', G', μ', and a plane strain system with constants E, G and μ. Then it may be shown that the substitution of

$$E' = \frac{E}{(1-\mu^2)} \quad , \quad G' = G, \text{ and}$$
$$\mu' = \frac{\mu}{1-\mu} \, , \tag{36}$$

into the stress-strain relations for plane stress yields the equations for plane strain. Similarly, the substitution of

$$E = E' \frac{(1+2\mu')}{(1+\mu')^2} \quad , \quad G = G' \quad , \text{ and}$$
$$\mu = \frac{\mu'}{1+\mu'} \, , \tag{37}$$

into the stress-strain relations for plane strain yields the equations for plane stress. The equilibrium equations in terms of stress are identically equal and by inspection of Eqs. (13) and (18), it is seen that the compatibility equations also become identical if the above substitutions are made.

Thus a free slice and a constrained slice, which have the same physical dimensions and the same boundary loading, will have the same stress distribution if the Poisson's ratios of the two materials are related as shown above and if the moduli of elasticity are directly proportional. It is of interest to note that the free slice - constrained slice relations between the

18. "Graphostatics of Stress Functions", by H. M. Westergaard, Transactions ASME, Vol. 56, No. 3, 1934, p. 141.
19. "Handbook of Experimental Stress Analysis", edited by M. Hetényi, Chapter VII on "Analogies", by R. D. Mindlin and M. G. Salvadori, J. Wiley and Sons, 1950.

elastic constants for this point-isotropic material are the same as those for the case of homogeneous isotropic materials in which the stress distribution is dependent on the elastic constants. (see footnote 17, p. 762).

From Eq. (36) it is seen that practical use of this free slice-constrained slice analogy is limited to a certain range of values for Poisson's ratio. If the value in the plane strain system is 1/3, then the corresponding value for plane stress is 1/2. Since it is impossible for a material to have a value of Poisson's ratio of greater than 1/2, the limiting value for the analogy is $\mu = 1/3$, (plane strain), corresponding to $\mu' = 1/2$, (plane stress).

Now consider a semi-infinite thin free slice, subjected to a given boundary loading, whose thickness (h) is a function of the depth (z). The thickness is assumed to vary gradually, so that the state of stress may be considered two-dimensional. The equations of equilibrium of an infinitesimal element of this slice may be written as,

$$\left.\begin{aligned} &\frac{\partial(h\sigma_z)}{\partial z} + \frac{\partial(h\tau_{xz})}{\partial x} = 0 , \\ \text{and}\quad &\frac{\partial(h\sigma_x)}{\partial x} + \frac{\partial(h\tau_{xz})}{\partial z} = 0 . \end{aligned}\right\} \qquad (38)$$

The stress-strain relations may be written,

$$\begin{aligned} \varepsilon_x &= \frac{1}{E}(\sigma_x - \mu'\sigma_z) \\ &= \frac{1}{Eh}(h\sigma_x - \mu' h\sigma_z), \quad \cdots (x,z) \\ \gamma_{xz} &= \frac{\tau_{xz}}{G} = \frac{2(1+\mu')}{Eh}(h\tau_{xz}), \end{aligned} \qquad (39)$$

and the compatibility relation is given in Eq. (15). By use of Eqs. (15), (38), and (39), the compatibility equation for the variable thickness slice is given in terms of stresses as:

$$\begin{aligned} &\Delta(h\sigma_x + h\sigma_z) - 2\frac{\partial}{\partial z}(h\sigma_x + h\sigma_z)\frac{\partial \ln h}{\partial z} \\ &+ (h\sigma_x - \mu h\sigma_z)\left[\left(\frac{\partial \ln h}{\partial z}\right)^2 - \frac{\partial^2 \ln h}{\partial z^2}\right] = 0 \end{aligned} \qquad (40)$$

By comparing Eq. (40) with Eqs. (13) and (18), and by comparing the equilibrium equations, it is seen that the two systems are mathematically identical, except for the boundary conditions, if one identifies:

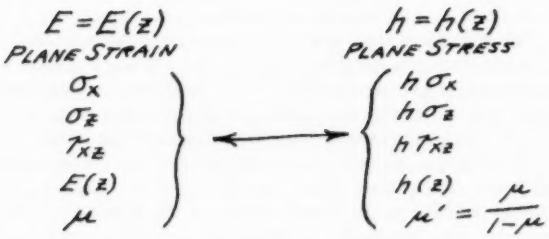

(41)

Therefore, if a semi-infinite free slice with varying thickness is loaded on the top surface, the stress multiplied by the thickness at a given point is equal to the stress at a corresponding point in a semi-infinite constrained slice of varying modulus, loaded similarly, providing that the relations of Eq. (41) are maintained. Thus the analogy is proved mathematically. It should be noted that in the compatibility relation, it is merely the derivatives of the ln G and ln h terms which must correspond, so that the thickness of the free slice may be scaled geometrically to any desired value.

Since it is obviously impossible to test a semi-infinite slice, either photoelastically or otherwise, a finite model must be used. Durelli[20] and Frocht[21] have used relatively small sheets of Bakelite as photoelastic models to check the Flamant solution for the semi-infinite plate. Away from the edges of the model, the results checked very well with theory. Thus, by comparing the stress distribution in two plates of the same size under the same load, one plate having a constant thickness and the other having a variable thickness, it appears possible to determine by use of this analogy the effect a variable modulus has upon the stress distribution caused by infinite line or strip loads.

The photoelastic method provides a means of determining at each point in the model, (a) the difference of the principal stresses, from the fringe patterns, and (b) the direction of the principal stresses, from the isoclinics. For a complete study of the stress distribution, it is also necessary to determine the sum of the principal stresses at each point. This may be done by any one of the usual methods.

For this type of problem it appears that a numerical method will prove to be the most expedient since the models will have rectangular boundaries. The boundary conditions will consist of a load applied at a point, or distributed over a small area, on the top edge of the plate and a known or assumed distribution of stress on the bottom edge. The vertical edges of the plate will be free from external loads. A comparison is to be made between the stress distribution in the plate of constant thickness and that in the plate whose thickness varies with depth.

For the case of the constant thickness plate, the photoelastic fringe pattern will determine the values of the difference of the principal stresses (p - q) at each point of the model by the relation:

20. "Distribution of Stresses in Partial Compression and...", by A. J. Durelli, Proc. 13th Semi-annual Eastern Photoelasticity Conference, June 1941, p. 15.
21. "Photoelasticity", by M. M. Frocht, Vol. II, J. Wiley and Sons, Inc., N. Y., 1948.

$$\frac{p-q}{2} = \frac{f \cdot n}{h} \quad , \tag{42}$$

in which n is the fringe order,
f is the material fringe constant,
and h is the thickness of the model.

On the free boundary, p + q equals p - q, so that the fringe pattern also determines the boundary stress values. The singularity due to the concentrated load on the top surface may be eliminated in the usual way by considering a small semi-circular groove to be cut out under the load. Then the surface of the groove is assumed to be subjected to an equipollent radial stress distribution as given by the Flamant solution. The stress distribution along the base of the model will be determined by the method of supporting the model. The boundary values of (p + q) as established above, and the compatibility relation,

$$\Delta(p+q) = 0 \tag{43}$$

which results from Eq. (40) for a constant thickness plate, are sufficient for the solution of the stress distribution by the iteration or relaxation methods. The finite difference net for use with such numerical methods is shown in Fig. 3.

Now consider the case of the photoelastic model having a variable thickness. Eq. (42) may be rewritten as,

$$\frac{h(p-q)}{2} = fn \tag{44}$$

and the compatability equation to be satisfied is given by Eq. (40) if h(p+q) is substituted for $h(\sigma_x\ \sigma_z)$. The boundary values of h(p+q) are established in the same manner as for the constant thickness model. In order to solve Eq. (40), it is necessary to express $(h\sigma_x - \mu h\sigma_z)$ in terms of h(p+q) and other known quantities. By introducing the angle, α, between the z-axis and the direction of the principal stress, p, Eq. (40) becomes,

$$\begin{aligned} &\Delta(hp+hq) - 2\frac{\partial}{\partial z}(hp+hq)\frac{\partial \ln h}{\partial z} \\ &+\left[\left(\frac{1-\mu}{2}\right)(hp+hq)\right. \\ &\left. -\frac{1+\mu}{2}(hp-hq)\cos 2\alpha\right]\left[\left(\frac{\partial \ln h}{\partial z}\right)^2 - \frac{\partial^2 \ln h}{\partial z^2}\right] = 0 \end{aligned} \tag{45}$$

The only unknown in Eq. (45) is h(p+q) at interior points, since the values of α are known from the isoclinics, and h(p-q) is known from the fringe pattern. Thus, Eq. (45) may be solved numerically and the complete stress distribution in the model may be obtained.

Figure 3 shows Eq. (45) in the finite difference form for a square net. If the variation of thickness is not easily expressed analytically, the required derivatives may also be obtained graphically or by the use of finite differences.

Selection of Photoelastic Model

The analogy has been proved mathematically, but it is still necessary to evaluate its suitability as a tool for experimental stress studies.

The first consideration must be the choice of a photoelastic model which corresponds by analogy to a given variation of elastic modulus in the semi-infinite body. Of the known solutions discussed, the only one which is valid for any given value of Poisson's ratio is Borowicka's solution using E = kz. The photoelastic model which represents this modulus has a thickness which corresponds to h = kz, or a wedge. The obvious difficulties encountered in applying load to the sharp edge of a wedge are partially offset by the simple machining operations involved in preparation of the model.

After a consideration of the photoelastic behavior, machinability, and availability of the various materials ordinarily used for photoelastic models, Bakelite BT 61-893 was selected for the wedge. The material fringe value was found by use of standard tension specimens to be 44.3 psi. shear per fringe per inch thickness for the 1/2 inch thick plate, and 41.5 psi. shear per fringe per inch for the 1/4 inch thick plate. Poisson's ratio of this material was found to be 0.366 from lateral and longitudinal strain measurements on a tension strip. The longitudinal strains were measured with two 1 inch gage length Huggenberger strain gages and the lateral strains were measured by use of a Vose Interferometer[22] strain gage.

After selection of a suitable material for the photoelastic model, the physical dimensions of the model were chosen. Since the test was to simulate the behavior of a semi-infinite plate, it is obvious that the height-width ratio of a finite model will have an important effect on the stress distribution. Previous studies[23] have shown that the theoretical fringe pattern produced by a line load acting on a semi-infinite plate, consists of circles tangent to the top surface at the point of loading. Thus a theoretical fringe would be tangent to the four sides of a square cut out of the plate. However, a photoelastic model is usually supported along the base, which could be considered to act as extending the model. In addition, the vertical sides of loading can be expected to have a greater effect on the stresses in the neighborhood of the load than does proximity of the base. This leads to a model wider than it is high. A series of tests was conducted to determine the most desirable height-width ratio for a plate loaded by a concentrated load and supported by a distributed reaction. From these tests a height-width ratio of 0.60 was chosen.

In order to derive full information from the use of the photoelastic analogy, it is very important that the "stress concentrating" effects due to the variable thickness are separated from those effects introduced by the boundary conditions of geometry and stress distribution. An analysis of the effect of these boundary conditions was made during this investigation.

The next step is to determine a suitable height and thickness for the

22. "An application of the Interferometer Strain Gage in Photoelasticity", by R. W. Vose, Journal of Applied Mechanics, Trans. ASME, Vol. 2 No. 3, September 1935, p. A-99.
23. See Footnote 5, p. 85.

model. The overall size is usually limited by the size of the polariscope field, unless a movable loading frame is devised so that an overlapping photograph technique could be used. However, the primary consideration is to design a model so that the best possible fringe count is obtained over the whole area. Increasing the thickness increases the fringe count, for a given stress, but this simple answer is counteracted by the necessity of maintaining a thin enough model to preserve a two-dimensional stress system. A wedge angle of about 14° was found to be satisfactory for such models. The useful height of the wedge is determined by the fringe count which may be obtained. From Eqs. (41) and (44), it is seen that the maximum shear for the analog is given by the value of (nf) at each point of the model. Thus the fringes, or lines of constant n, are expected to be approximately circular as for the plate, and of approximately the same size for the same total load. The total load on the wedge is analogous to the line load on the point-isotropic medium. However, since the edge of the wedge can support only a rather small load, the height of the model is limited to a value such that fringes are obtained over the whole model. Preliminary experimentation lead to the choice of a height of 0.90 inches.

With regard to the top surface of the model, it is also obvious that a thickness of zero would develop infinite stress under any load. Consequently, the edge would chip out, or flow plastically, even under small loads. Also this chipping effect would likely occur during machining of the Bakelite so it is doubtful if such an edge could be machined, even if it were desired. Preliminary experiments showed that a top thickness of about 0.020 inches was the best compromise between desire and possibility.

Experimental Procedure

The wedge was loaded along its plane of symmetry by a concentrated force acting on the top edge. The lower edge of the model rested on several thicknesses of cardboard. The cardboard rested on a Plexiglas block which in turn was supported by a steel block. Steel rollers were placed between the steel block and the steel base plate so as to eliminate any horizontal force which might be introduced by the loading device. The method of loading the models is shown diagrammatically in Fig. 4, and the actual test set-up is shown in Fig. 5. The load was applied through a lever system and was indicated by the deformation of a series of iso-elastic springs. This loading frame was calibrated in both tension and compression before starting the tests.

Since the wedge was loaded along its axis of symmetry, its faces were not perpendicular to the optical axis of the polariscope. Thus it was necessary to immerse the wedge in a liquid bath which had the same index of refraction as that of the model material. A satisfactory liquid was prepared by mixing one part of Bayol F White oil with two parts of Halowax 1007 oil. The container for the oil was made from sheets of 1/8 inch and 1/2 inch Plexiglas and is shown on Fig. 5.

In order to increase the fringe count obtainable for a given load per wedge, two wedges were placed parallel and loaded by a single pin. This procedure involved some question as to the distribution of load in each wedge, although the results obtained were found to agree well with later tests on single wedges. However, the difficulties involved in equalizing the loads, and also those of alignment made this set-up impractical; consequently a single wedge was used for all remaining tests.

The thin top edge of the wedge caused large stresses to appear in this region, even when relatively light loads acted. In order to obtain fringe values close to the load before the pin dug into the edge, photographs were taken of the fringe pattern for a series of increasing loads. Thus the values obtained are most accurate in the top portion of the model for small values of load and more accurate at lower depths for large values of load.

Tests were also run on plates of constant thickness, to evaluate the method of support of the base. A plate of Bakelite 1.80 inches high by 1.50 inches wide was loaded by concentrated loads on opposite edges, thus simulating the problem of a layer of finite thickness on a slippery rigid base, (Fig. 6c). In the next test, a block was loaded as shown in Fig. 6d. This test is analogous to the problem of two elastic layers on a rigid base, assuming (a) the interface between elastic layers is perfectly adhesive, and (b) the surface of the rigid base is slippery, thus developing no shear stress. At the increase of thickness, the stress distribution is certainly not two-dimensional, but if a small region on each side of the jump in thickness is excluded, the stress distribution is analogous to the layered system problem.

Figs. 6a, 6b, 6c, and 6d, show the various models employed, and Figs. 7 to 12 show representative fringe patterns.

Sources of Error in the Photoelastic Method

The results obtained are subject to the usual errors of the photoelastic method, in addition to the errors peculiar to this particular investigation which have been mentioned. However, due to the special precautions, as noted below, it was felt that the usual errors were kept to a minimum.

Time-edge effects in the models were practically eliminated by keeping the models in a bath of Halowax oil. In addition, since no boundary fringes were used as a basis for calculations, there was no cause for such edge effects to be serious.

Machining stresses were kept to a minimum by making very light cuts during the last few passes. The unloaded models showed no fringes, and a uniform intensity of light when seen in the polariscope.

The fringe patterns obtained show that creep was probably insignificant, since the width of the bands was in keeping with the stress-gradients.

The fringe patterns for the models tested in the oil bath were somewhat fuzzy due to a certain amount of diffusion of light in the oil. This also blurred the edges slightly so that it was necessary to be very careful in measuring the fringe position.

Test Results from the Constant Thickness Plate

The value for the difference of the principal stresses (p-q) at each point in the plate may be computed from Eq. (42). By dividing the right side of this equation by $\frac{P}{h}$ to obtain the stresses due to a unit line load, the equation becomes,

$$\frac{p-q}{z} = \frac{f \cdot n}{p} \qquad (46)$$

The position of the fringes on the z-axis was obtained from the photographs and was designated in percent of the model height. Photographs were taken with both dark and light backgrounds for each load, so that both the

integer and half order fringes were obtained. For all tests, the fringes were discarded which corresponded to a maximum shear stress greater than the fringe elastic limit, assumed to be 3500 psi. shear. The values of (p-q) from tests and theory were then plotted for corresponding values of percent model height, as shown on Fig. 13.

From Fig. 13, it is seen that the test values of (p-q) are within about 5% of the theoretical values in the region between 8 and 30 percent of model height. The values are low at 8 percent, high at 30 percent, and in good agreement at about 15 percent of model height. The values are low near the top region of the plate due to the plastic flow under the pins which caused a redistribution of the stresses. For the lower region of the plate, the stresses are high due to the shape of the model, and method of support.

Test Results from the Wedge

By use of the analogy, the values of h(p-q) in the wedge were to be compared with the value of (p-q) obtained from Borowicka's solution using the value $\mu = 0.268$, (obtained from Eq. (37), using $\mu' = 0.366$ for the Bakelite). By integration of Borowicka's solution so as to give the solution due to an infinite line load, the value for the difference of the principal stresses was found to be,

$$(p-q) = \frac{2P}{\pi z} \cdot 1.225 \qquad (47)$$

This corresponds to an increase of 22.5% over the value obtained for the constant modulus of elasticity.

If the wedge is loaded by a total load of P pounds, then the values of h(p-q) obtained correspond to the values of (p-q) due to a line load of P pounds/unit length in the point-isotropic material. The values for a unit line load are again given by Eq. (46).

It is seen in Figs. 9 and 10, that the loading pin has dug into the top of the wedge considerably, so that the load is no longer concentrated at a point. In order to correct for this, it was assumed that the load on the top surface was distributed parabolically over the bearing width. As it was desired to compare the results for several wedges and loads, and thus different bearing widths, the correction was applied to the experimental values rather than to the theoretical values. To obtain a correction factor, the ratio of (p-q) for a parabolic distribution of load to (p-q) for a concentrated load on the z-axis was calculated, assuming the radial stress distribution for $E = kz$ and $\mu = 1/3$. (Table 3). Fig. 14 shows the plot of this ratio as a function of the angle β, where 2β is the angle subtended by the load at the point under consideration.

The experimental values of (p-q) given by Eq. (46) were then divided by the factor read from Fig. 14, and plotted against percent of model height as shown in Fig. 15. The theoretical values of (p-q) for the constant modulus and for $E = kz$ are also plotted on this figure.

The test results for the wedge, corrected for spreading of the load, are lower than the theoretical solution in the upper 45 percent of the model height. In Fig. 15 no curve was drawn through the experimental values. However, a curve through the average of the plotted points indicates variations from theory (curve I) of 4, 6, 5, and 4 percent at 10, 15, 20, and 30 percent of model height, respectively. The scatter of results is considerably

larger than was obtained using the constant thickness models. This is due to the following three factors: (a) the small loads applied to the wedge were not measured as accurately by the loading frame, (b) the fringe count is much lower than in the plate, therefore any residual stresses in the model become more significant, and (c) the lower stress gradient produces broader fringes so that location of their mid-position is more subject to personal errors.

These results for (p-q) on the axis of the wedge are not too satisfactory, due to the rather large correction factor required to account for the distribution of the load. However, an additional corroboration of the analogy was obtained by comparing the shape of the fringes to the shape of the theoretical fringe. This was done for fringes in the region of the wedge which corresponds to the region of the constant thickness plate for which the fringes are circular. Since the stress distribution for $E = kz$ and $\mu = 1/3$ is not much different than that for $\mu = 0.268$, the fringes in the wedge were compared with the theoretical shape for $\mu = 1/3$. For this solution, it is shown in Table 3 that σ_μ is the only principal stress not equal to zero and as a result, the expression for (p-q) is given as,

$$\sigma_r = (p-q) = \frac{3q}{4}\frac{\cos^2\theta}{r} \tag{48}$$

Therefore the theoretical fringes are lines denoting,

$$\frac{\cos^2\theta}{r} = \text{a constant}. \tag{49}$$

Fig. 16 shows a theoretical fringe determined by Eq. (49) and a circle which corresponds to the theoretical fringe for a constant thickness plate. The plotted points indicate the shape of fringes in a wedge 1.50 x 0.90 inches, 0.014 inches thick at the top, obtained for loads of 20.6 and 41.2 pounds. The experimental and theoretical shapes are seen to be in close agreement except very near to the top surface, where the spreading of the load again caused fringe distortion. This correspondence between the theoretical and test fringe shapes is thus considered to be an acceptable confirmation of the mathematical analogy.

Conclusions

The problem of the stress distribution in a semi-infinite body due to surface loading has been analyzed for certain non-homogeneous materials. It was assumed that the material is isotropic at any particular point and that Poisson's ratio is constant throughout the region, but that the modulus of elasticity is a function of depth beneath the top surface, although constant at any given depth. This is called a point-isotropic material.

The general equations of elasticity for such a material have been derived for a general variation of the modulus, and the known solutions due to Fröhlich, Ohde, and Borowicka have been examined with regard to their validity and limitations. It was shown that superposition of the correct solutions is permissible.

There is shown to be a mathematical analogy between the stress distribution in a semi-infinite body of point-isotropic material due to line or strip loads, and the stress distribution due to similar loads in a semi-

infinite plate of homogeneous isotropic material. The thickness of the plate must vary with depth in a manner corresponding to the modulus variation in the point-isotropic material. Thus it becomes possible to use the photoelastic method to determine stresses in point-isotropic materials.

The mathematical analogy is confirmed experimentally by use of a wedge-shaped photoelastic model. This was analogous to a point-isotropic material for which the modulus of elasticity increased linearly with depth from a zero value at the top surface.

Since the variation in modulus may cause stress distributions appreciably different from those obtained for the homogeneous isotropic materials, its effect may be interpreted as a "stress concentration." Boundary conditions, such as rigid layers, or hydrostatic pressures, also affect the stress distributions in the overlying material, so that it is necessary to identify the contribution of each in the experimental work. It was also shown that the photoelastic method may be applied to certain problems of layered systems provided the results are recognized as inaccurate at the interfaces of the layers.

It is suggested that the photoelastic analogy may be used in two ways. In the first case, a complete stress distribution in the model may be obtained and compared with the complete stress distribution in a plate of similar size. In using such a comparison, considerations must be made with regard to the method of support and the stress concentrating effects induced thereby. For the second case, the ratio of (p-q) along the z-axis of the model to the value of (p-q) along the z-axis of a similarly supported plate is determined in the region between 10 and 20 percent of the model height. This ratio may then be used to obtain appropriate values of the stress concentration factor, n. This value of n may then be used in Fröhlich's equations to give an approximation for the stress distribution in the point-isotropic material. The validity of this method depends upon the relation between n, and the elastic constants of the material. However, if the approximation is reasonable, this method is convenient, since Fröhlich's equations may be integrated easily.

A limitation of the method is that solutions can be obtained only for values of Poisson's ratio between about 0.23 and 0.33, since presently available photoelastic materials have Poisson's ratios varying from about 0.30 to 0.50.

Acknowledgement

This study of the stress distribution in non-homogeneous materials, was undertaken at the suggestion of A. Casagrande, Gordon McKay Professor of Soil Mechanics and Foundation Engineering, Harvard University, whose many helpful suggestions are sincerely appreciated. The method of verifying the analogy, as represented in Figure (16), was suggested by C. E. Pearson, Instructor in Applied Mechanics, Harvard University.

The Division of Applied Science of Harvard University provided the materials and equipment for the experimental work involved in this study, except for the determination of Poisson's ratio of the Bakelite. This was carried out in the Experimental Stress Laboratory of the Massachusetts Institute of Technology, through the courtesy of Professor W. M. Murray and Mr. W. L. Walsh. The Department of Civil Engineering of the University of Florida assisted in the preparation of the manuscript.

TABLE 1

Vertical Stress Along Loading Axis in a Material for which E = kz

Poisson's Ratio μ	$\left(\frac{\sigma_z}{\frac{3P}{2\pi z^2}}\right)$ at $\rho = 0$
1/2	1.00
1/3	1.33
1/4	1.47
0	1.76

TABLE 2

Vertical Stress, σ_z, due to a Point Load P Acting Vertically at the Surface of the Semi-Infinite Body

E	μ	σ_z	$\left(\frac{z^2\sigma_z}{P}\right)_{\rho=0}$	σ_R
Const.	0 ← → 1/2	$\frac{3P}{2\pi}\frac{z^3}{R^5}$	0.477	$\frac{P}{\pi R^2}\left[(2-\mu)\cos\psi - \frac{(1-2\mu)}{2}\right]$
kz	1/2	$\frac{3P}{2\pi}\frac{z^3}{R^5}$	0.477	$\frac{3P}{2\pi}\frac{\cos\psi}{R^2}$
kz	1/3	$\frac{2Pz^4}{\pi R^6}$	0.637	$\frac{2P}{\pi}\frac{\cos^2\psi}{R^2}$
kz	1/4	Infinite Series	0.699	Infinite Series
kz	0	Infinite Series	0.839	Infinite Series
$kz^{1/2}$	0.40	$\frac{7P}{4\pi R^2}\cos^{\frac{7}{2}}\psi$	0.557	$\frac{7P}{4\pi R^2}\cos^{\frac{7}{2}}\psi$
kz^{ω}	$\frac{1}{n-1} = \frac{1}{\omega+2}$	$\frac{nP}{2\pi R^2}\cos^n\psi$	$\frac{n}{2\pi}$	$\frac{nP}{2\pi R^2}\cos^{n-2}\psi$

TABLE 3

Vertical Stress, σ_z, due to a Line Load of q/unit Length Acting Vertically at the Surface of the Semi-Infinite Body

E	μ	σ_z	$\left(\frac{z\sigma_z}{q}\right)_{x=0}$	σ_r
Const.	$0 \leftrightarrow 1/2$	$\frac{2q}{\pi}\frac{\cos^3\theta}{r}$	$\frac{2}{\pi}$	$\frac{2q}{\pi}\frac{\cos\theta}{r}$
kz	1/3	$\frac{3q}{4}\frac{\cos^4\theta}{r}$	3/4	$\frac{3q}{4}\frac{\cos^2\theta}{r}$
$kz^{1/2}$	0.40	$f_{(1/2)}^{*}q\frac{\cos^{\frac{1}{2}}\theta}{r}$	$f_{(1/2)}$	$f_{(\frac{1}{2})}q\frac{\cos^{\frac{3}{2}}\theta}{r}$
kz^n	$\frac{1}{n-1} = \frac{1}{n+2}$	$f^{*}q\frac{\cos^n\theta}{r}$	f	$f\cdot q\frac{\cos^{n-2}\theta}{r}$
$\frac{k}{z}$	$0 \leftrightarrow \frac{1}{2}$	$\frac{4q}{\pi^2}\frac{z\arctan\frac{z}{x}}{r^2}$	$\frac{2}{\pi}$	$\frac{4q}{\pi^2}\cdot\frac{1}{z}\arctan\frac{z}{x}$

*where $f = \frac{1}{2\int_0^{\frac{\pi}{2}}\cos^{n-1}\theta\,d\theta}$ and $f_{(1/2)} = 0.7218$

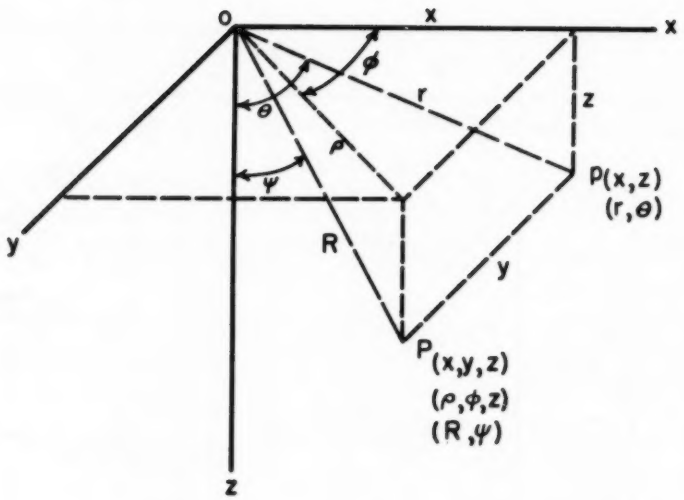

Fig. 1. Coordinate Systems

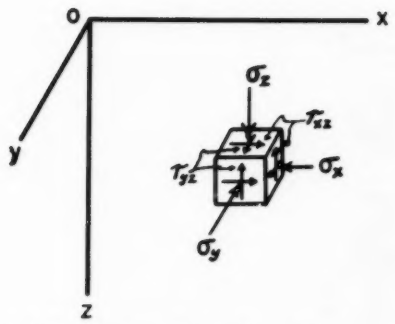

(a) Cartesian Coordinates
(three dimensions)

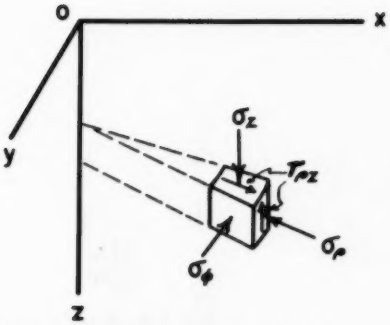

(b) Cylindrical Coordinates,
(axially symmetric)

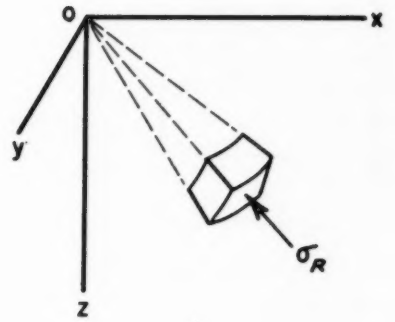

(c) Spherical Coordinates
(radial stress distribution)

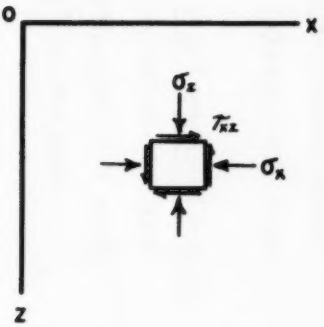

(d) Cartesian Coordinates
(two dimensions)

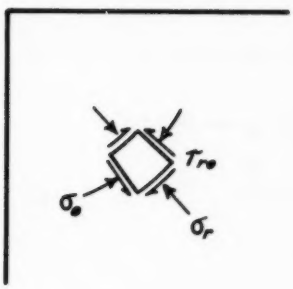

(e) Plane Polar Coordinates

Fig. 2. Conventions for Positive Stresses

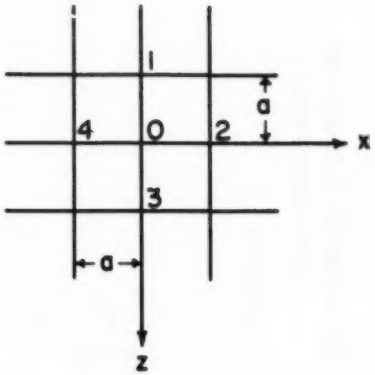

Constant Thickness Plate

$$4F(0) = F(1)+F(2)+F(3)+F(4)$$

where $F(n) = (p+q)(n)$

Varying Thickness Plate

$$A(0)F(0) = B(0)F(1)+C(0)F(3) + F(2) + F(4) - D(0)$$

where $F(n) = h(p-q)(n)$,

$$A(n) = 4 - a^2\frac{(1-\mu)}{2}\left[\left(\frac{\partial \ln h}{\partial z}\right)^2 - \frac{\partial^2 \ln h}{\partial z^2}\right]_n$$

$$B(n) = 1 + a\left[\frac{\partial \ln h}{\partial z}\right]_n$$

$$C(n) = 1 - a\left[\frac{\partial \ln h}{\partial z}\right]_n$$

$$D(n) = \left\{\frac{(1+\mu)}{2}(hp-hq)\cos 2\alpha\left[\left(\frac{\partial \ln h}{\partial z}\right)^2 - \frac{\partial^2 \ln h}{\partial z^2}\right]\right\}_n$$

Fig. 3. Square Net and Finite Difference Equations for (p + q)

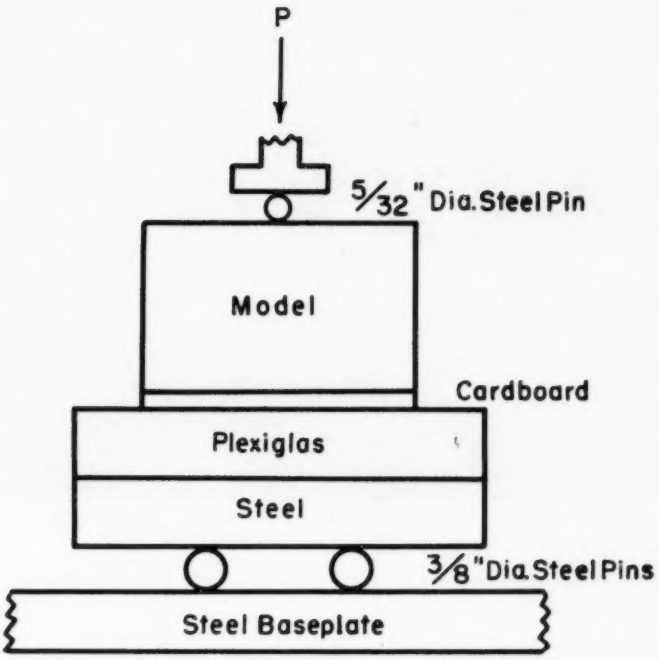

Fig. 4. Method of Loading Models

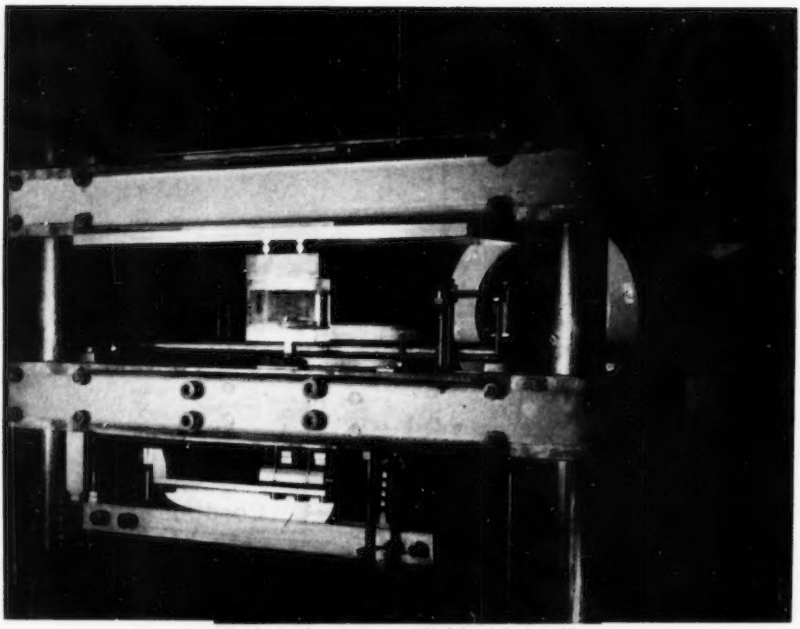

Fig. 5. Loading Frame with Model and Tank in Place

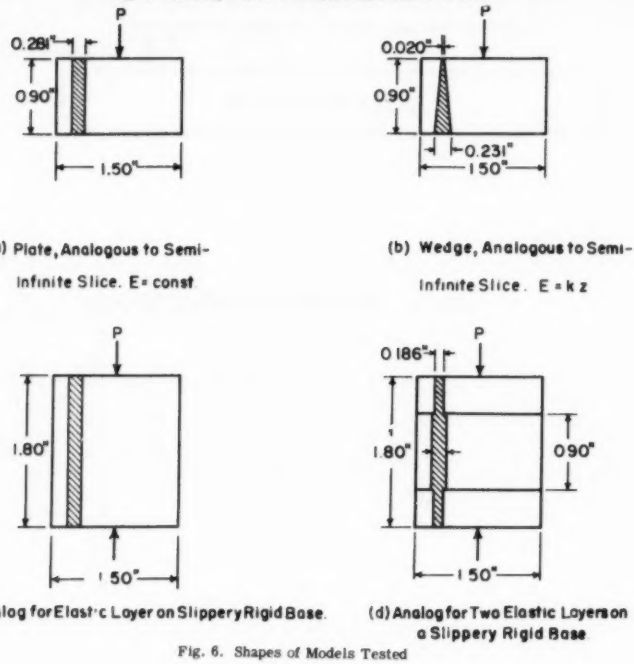

(a) Plate, Analogous to Semi-Infinite Slice. E = const

(b) Wedge, Analogous to Semi-Infinite Slice. E = k z

(c) Analog for Elastic Layer on Slippery Rigid Base.

(d) Analog for Two Elastic Layers on a Slippery Rigid Base

Fig. 6. Shapes of Models Tested

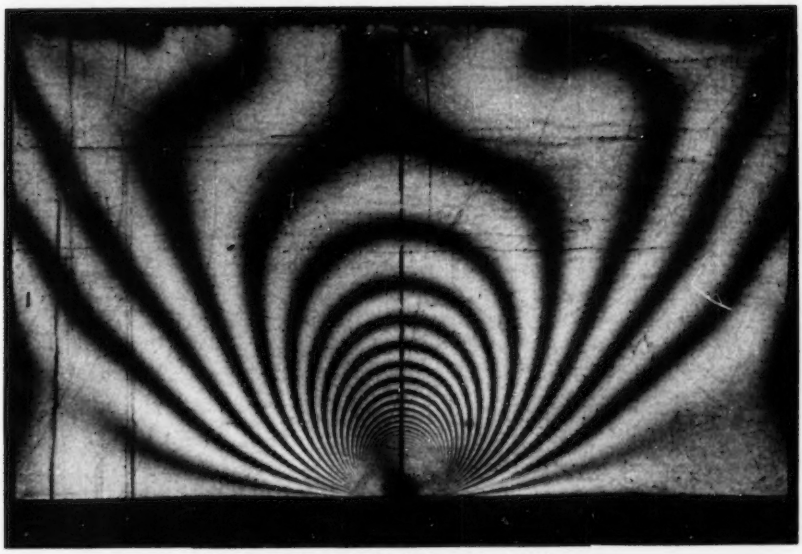

Fig. 7. Bakelite Plate (Fig. 6a) Under Load of 464 lbs.

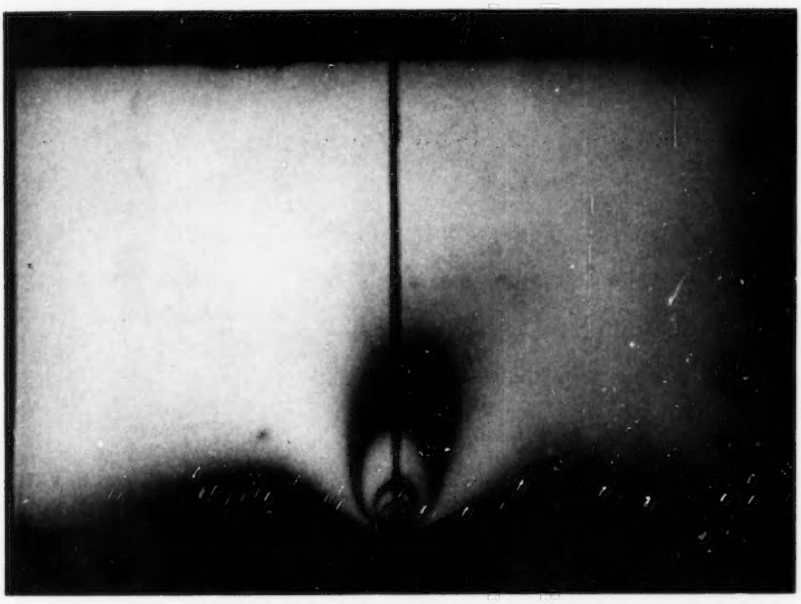

Fig. 8. Bakelite Wedge (Fig. 6b) Under Load of 20.6 lbs.

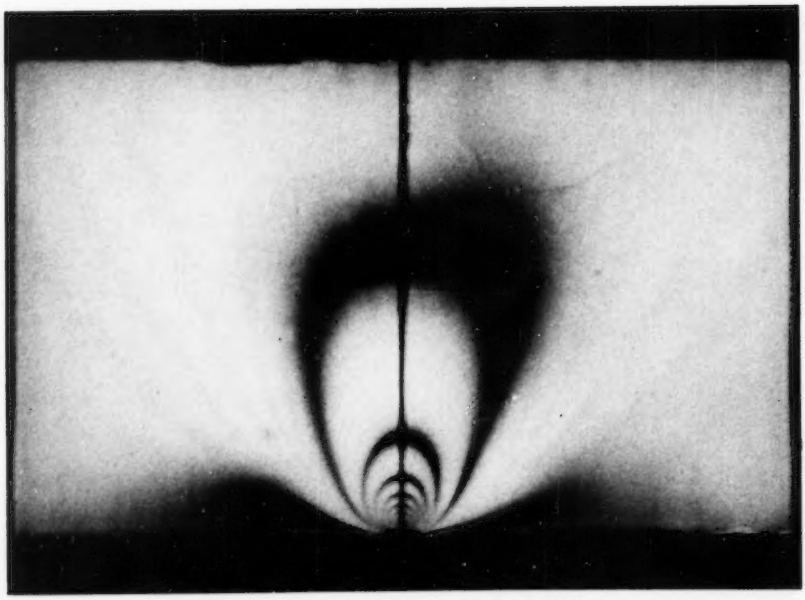

Fig. 9. Bakelite Wedge (Fig. 6b) Under Load of 41.2 lbs.

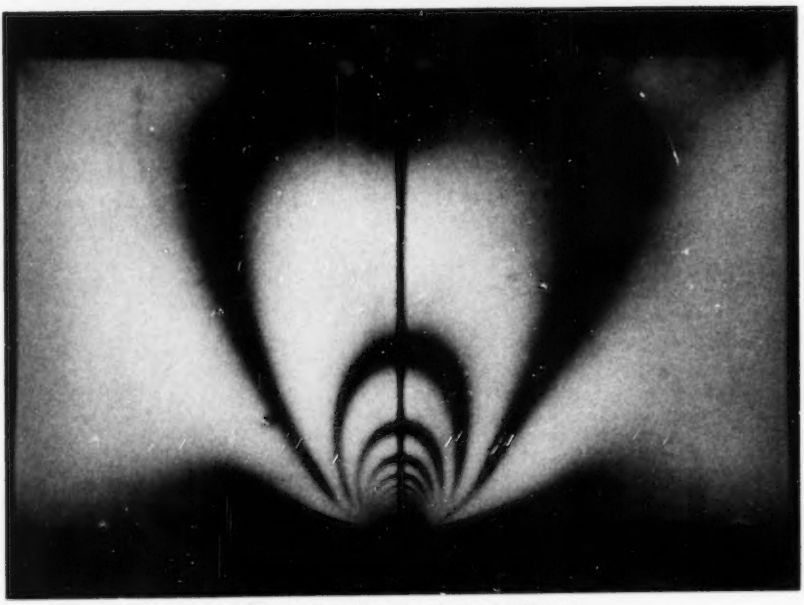

Fig. 10. Bakelite Wedge (Fig. 6b) Under Load of 72.1 lbs.

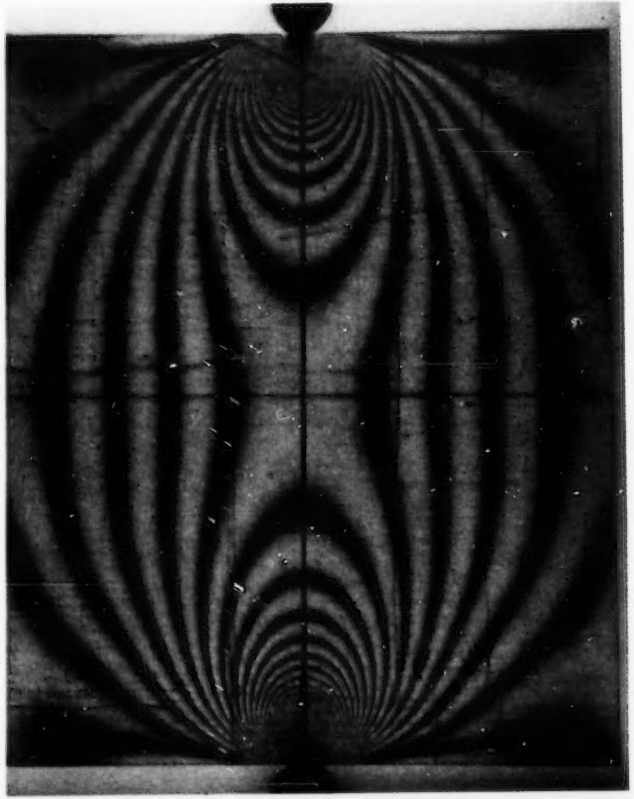

Fig. 11. Bakelite Plate (Fig. 6c) Under Load of 292 lbs.

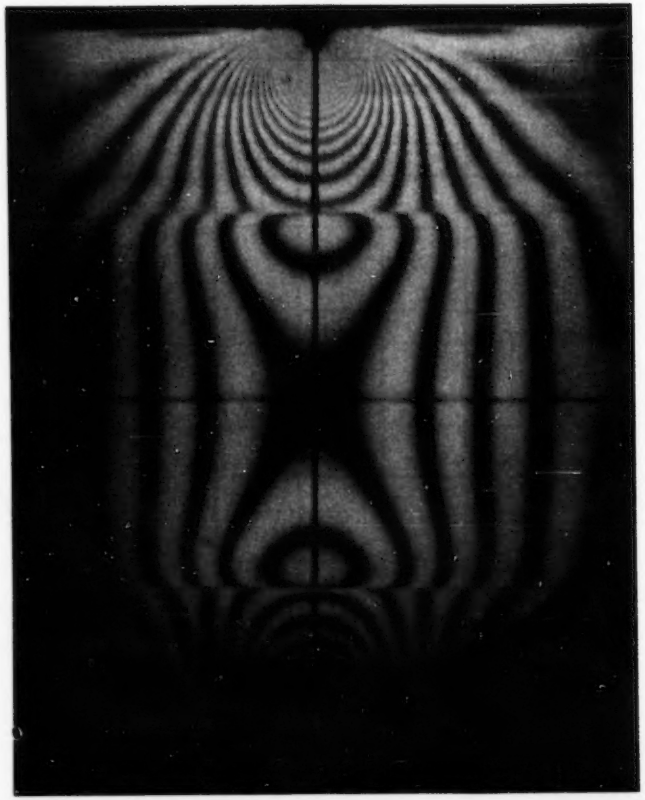

Fig. 12. Bakelite Plate (Fig. 6d) Under Load of 292 lbs.

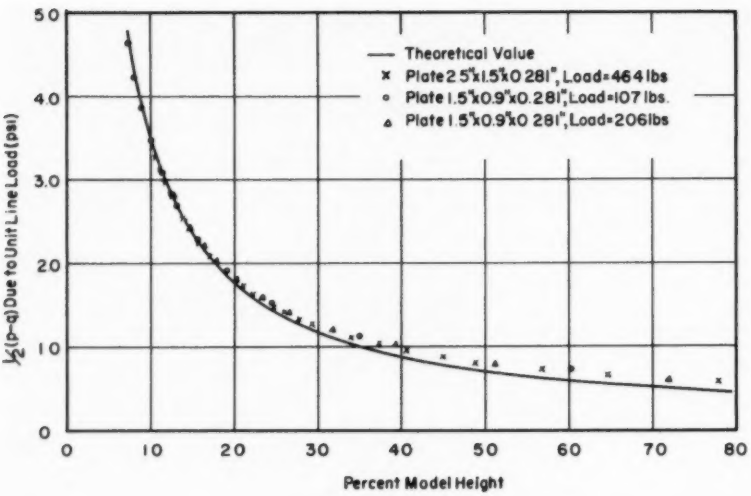

Fig. 13. Experimental and Theoretical Values of (p - q) along the Axis of Loading for the Plate Model

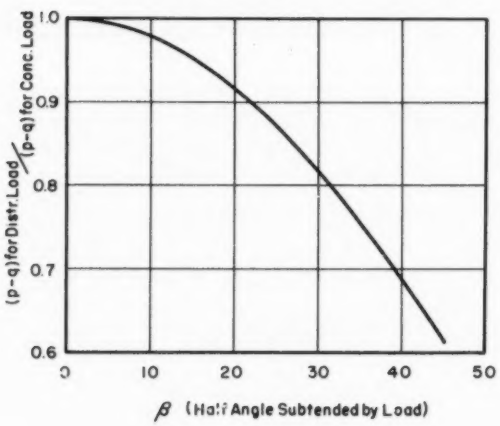

Fig. 14. Correction Factor for Parabolic Distributions of Load

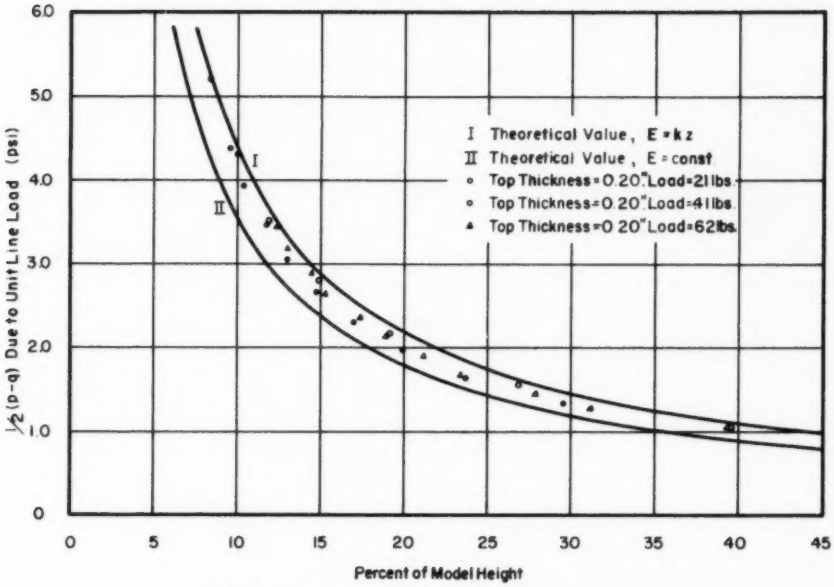

Fig. 15. Experimental and Theoretical Values of (p - q) along the Axis of Loading for the Wedge Models. (Analogous to $E = kz$ for $\mu = 0.268$)

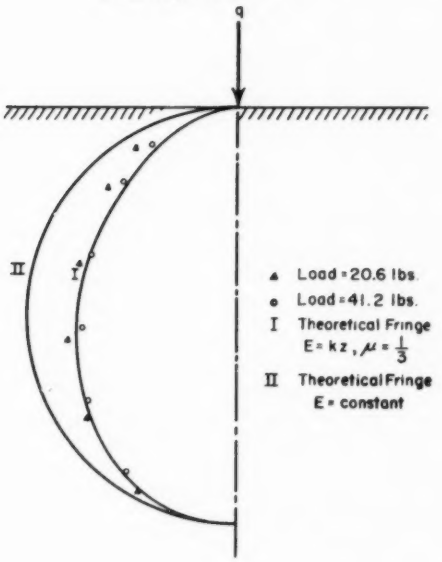

Fig. 16. Theoretical and Experimental Fringe Shapes for the Wedge Model

AMERICAN SOCIETY OF CIVIL ENGINEERS

OFFICERS FOR 1953

PRESIDENT

WALTER LEROY HUBER

VICE-PRESIDENTS

Term expires October, 1953:
GEORGE W. BURPEE
A. M. RAWN

Term expires October, 1954:
EDMUND FRIEDMAN
G. BROOKS EARNEST

DIRECTORS

Term expires October, 1953:
KIRBY SMITH
FRANCIS S. FRIEL
WALLACE L. CHADWICK
NORMAN R. MOORE
BURTON G. DWYRE
LOUIS R. HOWSON

Term expires October, 1954:
WALTER D. BINGER
FRANK A. MARSTON
GEORGE W. McALPIN
JAMES A. HIGGS
I. C. STEELE
WARREN W. PARKS

Term expires October, 1955:
CHARLES B. MOLINEAUX
MERCEL J. SHELTON
A. A. K. BOOTH
CARL G. PAULSEN
LLOYD D. KNAPP
GLENN W. HOLCOMB
FRANCIS M. DAWSON

PAST-PRESIDENTS

Members of the Board

GAIL A. HATHAWAY
CARLTON S. PROCTOR

TREASURER

CHARLES E. TROUT

EXECUTIVE SECRETARY

WILLIAM N. CAREY

ASSISTANT TREASURER

GEORGE W. BURPEE

ASSISTANT SECRETARY

E. L. CHANDLER

PROCEEDINGS OF THE SOCIETY

HAROLD T. LARSEN
Manager of Technical Publications

DEFOREST A. MATTESON, JR.
Assoc. Editor of Technical Publications

PAUL A. PARISI
Asst. Editor of Technical Publications

COMMITTEE ON PUBLICATIONS

LOUIS R. HOWSON

FRANCIS S. FRIEL
GLENN W. HOLCOMB
I. C. STEELE
FRANK A. MARSTON
NORMAN R. MOORE

• Readers are urged to submit discussion applying to current papers. Forty free Separates per year are allotted to members. Mail the coupon order form found in the current issue of *Civil Engineering.*